Physica A 391 (2012) 6390–6398

Contents lists available at SciVerse ScienceDirect

Physica A

journal homepage: www.elsevier.com/locate/physa

Configurational entropy of systems with non-additive lateral interactions

O.A. Pinto, A.J. Ramirez-Pastor, F. Nieto *

Departamento de Física, Universidad Nacional de San Luis, Instituto de Física Aplicada, INFAP, CONICET, Chacabuco 917, D5700BWS San Luis, Argentina

ARTICLE INFO

Article history:
Received 11 December 2011
Received in revised form 5 April 2012
Available online 20 July 2012

Keywords:
Monte Carlo simulations
Configurational entropy
Lattice gas systems
Non-additive interactions

ABSTRACT

The configurational entropy per site of a lattice gas model with non-additive interactions between adsorbed particles for square, triangular and honeycomb lattices is discussed in the present study. The model used here assumes that the energy which links a certain atom with any of its nearest-neighbors strongly depends on the state of occupancy in the first coordination sphere of that adatom. By means of Monte Carlo simulations in the canonical ensemble by following the algorithm of parallel tempering and the thermodynamic integration method the configurational entropy per site has been calculated. By analyzing the behavior of the configurational entropy per site, the different low-temperature-ordered phases are described. The dependency of the critical temperature of the system as a function of characteristic parameters of the model is established.

1. Introduction

In recent years the development and improvement of powerful experimental techniques for surface analysis on the atomic scale has substantially improved our knowledge about the energetic surface topography and the understanding of the mutual interactions between particles deposited on such surfaces. Systematic studies have encouraged the development of adequate refined atomistic models for describing the interaction energies between adsorbed particles. Such models are capable of including different kinds of energetic coupling in the statistical description of several thermodynamic processes taking place on solid substrates. The non-additivity of lateral interactions in fact reflects the role of triple (quadruple, etc.) interactions as corrections to cases where pair-wise interactions are not enough for describing experimental observations. In particular, the non-pair-wise (non-additive) interactions have been considered for explaining different experimental findings in surface science, especially in metal on metal interactions. For this kind of coupling, it is extremely important to understand the phenomena occurring on the surface of a metal. These multibody interactions have been studied in several systems such as H on Pd(100) [1], O on W(110) [2–4] and H on Fe(110) [5–7], just to name a few of them. The multibody interactions can be interpreted with the non-additivity concept, which means that the lateral energy between nearest-neighbor adsorbed particles depends on how many particles are present (or absent) in their environment. This situation has been reported in several experimental systems: (i) monolayer growth in a heteroepitaxial system with the presence of heterogeneities Ag/Au(100), Ag/Pt(100), Au/Pt(100), Au/Pd(100), Au/Ag(100), Pt/Ag(100), Pt/Au(100) and Pd/Au(100) [8,9] and (ii) the electrochemical phase formation, Ag on Au(111) and Au(100) [10–13].

In the standard lattice gas model where additive interactions are included, the symmetry between particles and vacancies has been preserved [14]. However, in several experimental arrangements, the behavior of the thermodynamic quantities and the phase diagram of the system have shown clear signals of non-equivalence between particles and vacancies. In fact, adsorption isotherms for methane, ethane, and other adsorbates on AlPO4-5 and SAPO-5 are clearly unsymmetrical around

* Corresponding author. Tel.: +54 2652 431080; fax: +54 2652 431080.
E-mail address: fnieto@unsl.edu.ar (F. Nieto).

0378-4371/$ – see front matter
doi:10.1016/j.physa.2012.06.041

half coverage [15–19]. In fact, for experimental systems where non-additive interactions are present, a phase diagram asymmetry has been reported [20]. These asymmetries can be obtained by using Hamiltonians with terms accounting for more complex ad–ad interactions. Surface restructuring is another example of a system where more complex ad–ad interactions take place [21–25]. Another evidence of non-additivity is the tendency to dimer formation. This fact is observed, for example, in the adsorption of Cu and Ni on W(110) with thermal desorption spectroscopy analysis [26].

Since the seminal studies of non-additive interactions, it was established that the non-additivity is able to modify the critical temperature of the phase transitions occurring in the systems. In recent years, much work has been done in this direction [27]. In fact, statistical mechanics of non-additive adsorbed monolayers has been the subject of analytical treatment by means of the mean-field approximation (MFA) [28–30] and quasi-chemical approach [31], being specially analyzed in the case of attractive interactions [29]. However, repulsive interactions also represent an interesting case because (a) experimental phase diagrams corresponding to many systems in the presence of surface restructuring are explained in terms of those interactions [32–34]; (b) the tendency to dimer formation, which seems to be relevant in several systems mentioned above, can be predicted on the basis of such kinds of coupling; and (c) a rich variety of non-symmetrical phase diagrams can be described.

The non-additivity concept has been applied to monomeric adsorption in lattice gas models with repulsive interactions where the adsorption thermodynamics was analyzed [31,32]. The authors were able to identify important results: (i) a rich variety of ordered structures were observed in the adlayer, (ii) the formation of "k-mers" (chains of monomers adsorbed on k adjacent lattice sites) at high coverage and (iii) the symmetry of particle–vacancy (strictly valid for additive interactions) is broken and, consequently, the adsorption properties (adsorption isotherms, differential heat of adsorption, etc.) are asymmetric with respect to half coverage. Similar results have been found in adsorption of monomers in nanotube bundles [33].

To be more specific, in Ref. [31], a Monte Carlo study of the adsorption of monomers with non-additive interactions on square lattices has been presented. Adsorption isotherm, adsorption energy and isosteric heat of adsorption were calculated by means of Monte Carlo simulation in the grand canonical ensemble. The main results can be summarized as:

(i) whether the non-additivity weakens the $c(2 \times 2)$ ordered phase (as compared to the additive case), it is possible to distinguish the presence of different low-temperature ordered phases depending on the surface coverage. These findings are corroborated by very wide plateaus in the adsorption isotherms, steps in the isosteric heat of adsorption and weak peaks in the thermodynamic factor.
(ii) the formation of "k-mers" is corroborated in a specific range of coverage and interactions. It is interesting to mention that the structures represented by "k-mer phases", like "dimer" or "tetrameric phases" are observed in experiments [26].
(iii) if the non-additivity tends to reinforce the $c(2 \times 2)$ phase, there exists evidence of the presence of a continuous phase transition from the $c(2 \times 2)$ structure to disorder around half coverage.

For a better description, in Fig. 1 the adsorption isotherms are shown for different degrees of non-additivity and a fixed low temperature (low temperature should be understood as lower than a critical temperature). The plateau width as well as the critical point depends on how strong are the non-additive forces. For other geometries, such as triangular and honeycomb lattices, the results are quite similar [32].

The main aim of the present paper is to analyze the dependence of the configurational entropy in the presence of non-additive interactions for several geometries (squares, triangular and honeycomb lattices) by means of Monte Carlo simulation and the thermodynamic integration method (TIM) in the canonical ensemble [34–40]. These techniques allow us to identify the formation of new ordered structure. TIM uses the energy of the system and calculates the configurational entropy via integration. Thus, the dependence of the critical temperature as a function of the non-additivity parameter can be estimated. The paper is organized as follows. In Section 2, the lattice gas model for non-additive interactions is presented. In Section 3, details of Monte Carlo simulations and TIM in the canonical ensemble are given. Results and discussion are presented in Section 4. Finally, the conclusions are drawn in Section 5.

2. The non-additive lattice model

Let us consider an idealized solid surface of either square, honeycomb or triangular symmetry. The minima of the potential on the surface form a two-dimensional array with constant a, and coordination number z (=4 for square, 3 for honeycomb and 6 for triangular array). The considered surface will be a homogeneous potential surface "*as seen*" by an adsorbed particle. It is supposed that each adsorption site can be occupied only by one particle; the multiple occupation of sites is excluded. In fact, the Hamiltonian can be described by:

$$H = -\varepsilon \sum_{i=1}^{N} c_i - \sum_{\langle i,j \rangle}^{N} w_{ij} c_i c_j \tag{1}$$

where i and j denote the adsorption sites and the local occupation variable c_i is 0 (1) if the adsorption site is empty (occupied). ε reflects the interaction between the substrate and the adatoms, being independent of temperature and coverage (in the simulations, ε can be considered equal to zero without losing generality). The adsorbate–adsorbate interaction, w_{ij}, is

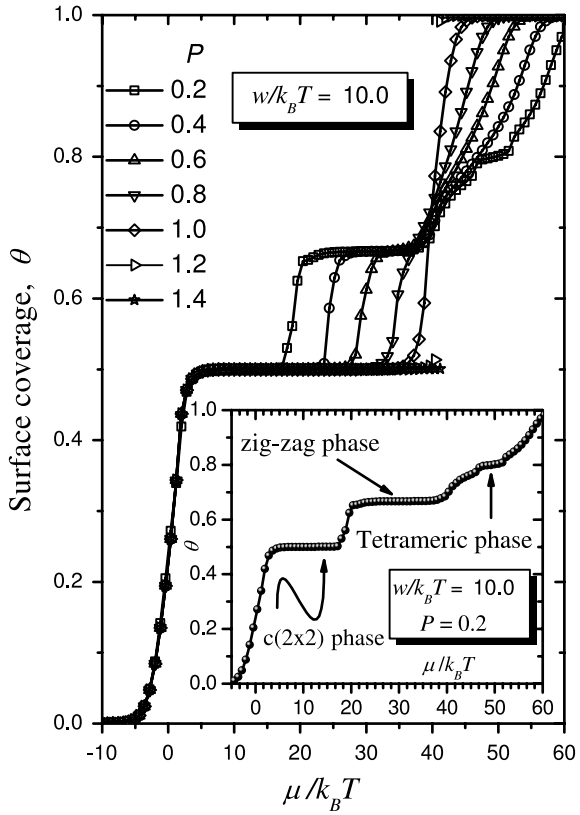

Fig. 1. Adsorption isotherms of monomers on square lattices for a fixed temperature ($w/k_BT = 10$) and different values of the non-additivity parameter P, as indicated. The inset shows the adsorption isotherm for $P = 0.2$ where the plateaus are clearly identified and associated to the different low-temperature ordered phases.

assumed to depend on the occupation state of the surroundings of a given site i. Following the lines of the thinking presented in previous works [31,32], the simplest non-additive interaction energy is considered. We assume that w_{ij} have different possible values w_m ($m = 1, 2, \ldots, z$) depending on how many first neighbors are actually present in the vicinity of a given atom. The case where w_m varies linearly with m and $w_z = w$ is considered. Following Refs. [28,29], a non-additivity parameter is introduced, $P = w_1/w_z$, as a measure for the stronger to the weakest bond possible in each system:

$$\frac{w_m}{w} = \frac{Pz - 1}{z - 1} - m\frac{P - 1}{z - 1}. \tag{2}$$

3. Monte Carlo simulation and thermodynamic integration method in canonical ensemble

Let us consider a lattice gas of N interactive particles, each of which can only occupy a single empty site on an array of M sites, at temperature T. The entropy S, can be written as:

$$\left(\frac{\partial S}{\partial T}\right)_{M,N} = \frac{1}{T}\left(\frac{\partial U}{\partial T}\right)_{M,N} \tag{3}$$

where U represents the internal energy and

$$S(N, M, T) = S(N, M, T_o) + \int_{T_o}^{T} \frac{dU}{T}. \tag{4}$$

By using the last expression, the entropy at the equilibrium state can be calculated. This procedure is called thermodynamic integration. The reference state $S(N, M, T_0)$ is trivial to be known:

$$\lim_{T_o \to \infty} S(N, M, T_o) = k_B \binom{M}{N} = k_B \ln\left[\frac{M!}{N!(M - N)!}\right] \tag{5}$$

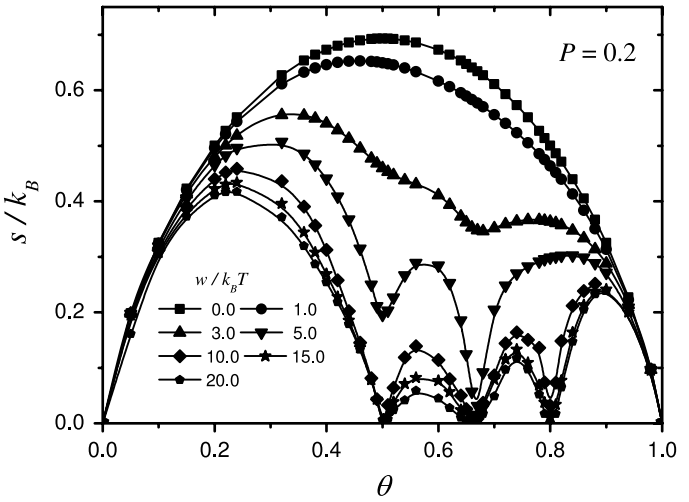

Fig. 2. Configurational entropy per site for monomers adsorbed on square lattices, $P = 0.2$ and different values of w/k_BT, as indicated.

where k_B is the Boltzmann constant. By using Stirling's approximation in Eq. (5), one can obtain:

$$\frac{s(\theta, T_o \to \infty)}{k_B} = -\theta \ln \theta - (1-\theta)\ln(1-\theta) \tag{6}$$

where $s = S/M$ is the entropy per site.

On the other hand, the integral in Eq. (4) can be evaluated by using Monte Carlo (MC) simulation. For this purpose, an adsorption–desorption algorithm is performed in the canonical ensemble applying the method of parallel tempering or replica exchange. This technique is useful for models with slow dynamics because the system is able to escape from local minima faster. The characteristic times to escape from these minima grow rapidly as the temperature decreases and upon increasing the size of the system [41–45].

The main idea of parallel tempering consists in simulating R replicas of the original system where each replica is simulated at different temperatures. The temperature range includes both phases of high and low temperature. Parallel tempering allows the exchange of systems at different temperatures generating a good sampling of the phase space.

Each attempt of changing the configurational state of the system is performed simultaneously for each one of the R replicas by using in each case a convenient transition probability which obviously depends on the temperature of the sample. As a consequence, such a simulation of R replicas requires R times more computational effort, but the parallel tempering makes $1/R$ times more efficient than a standard MC simulation. The method consists of two procedures. The first one, a standard MC method is used to simulate each replica which is updated by using the Metropolis rule [43]. In the second one, a trial exchange of two configurations X_n and X_m (corresponding to the n-th and m-th replicas) is attempted and accepted with probability:

$$W\,(X_n\beta_n/X_m\beta_m) = \begin{cases} 1 & \text{for } \Delta < 0 \\ \exp(-\Delta) & \text{for } \Delta > 0 \end{cases} \tag{7}$$

where $\Delta = (\beta_m - \beta_n)\,[H(X_n) - H(X_m),\,]$ and H is the Hamiltonian of the replica, and $\beta_{m(n)} = 1/k_BT_{m(n)}$. The temperature range $(T_m - T_n) = (T_{\text{high}} - T_{\text{low}})/(R-1)$ includes the phases of high temperatures and low temperatures. Following Ref. [46], the replica exchange is restricted to the case $m = n+1$. The way of combining the number of elementary steps of standard MC and the number of replica exchanges is as follows. The simulation starts with a random initial condition; a few MC steps (MCSs) of standard MC are applied to replica 1 (each MCS consists of M elementary steps of standard MC). The same procedure is done successively for each replica but taking the last configuration of replica m as the initial condition of replica $m+1$. A parallel tempering step (PTs) is defined as $M \times R$ cycles, each cycle being one elementary step of standard MC plus one replica exchange. After those cycles, the algorithm stops, then the observables are calculated. The approximation to thermodynamic equilibrium is usually reached in 10^6 PTs. Then, mean values of the internal energy, U, are obtained by averaging over 10^6 PTs configurations. Then, $U(T)$ is numerically integrated.

4. Results and discussion

The entropy per site in the case of non-additive repulsive interactions between adparticles on a square lattice is analyzed in the first place. By using lattice sizes larger than $L = 128$, it was verified that size effects are negligible. The dependence of the entropy on the temperature is discussed first. In fact, Fig. 2 shows the entropy for different values of temperature in units of w/k_BT, for a particular non-additive situation, $P = 0.2$ as indicated. For all temperatures considered, in the limit $\theta \to 0$ ($\theta \to 1.0$), the entropy tends to zero as expected. At very high temperature, the entropy is symmetric with respect

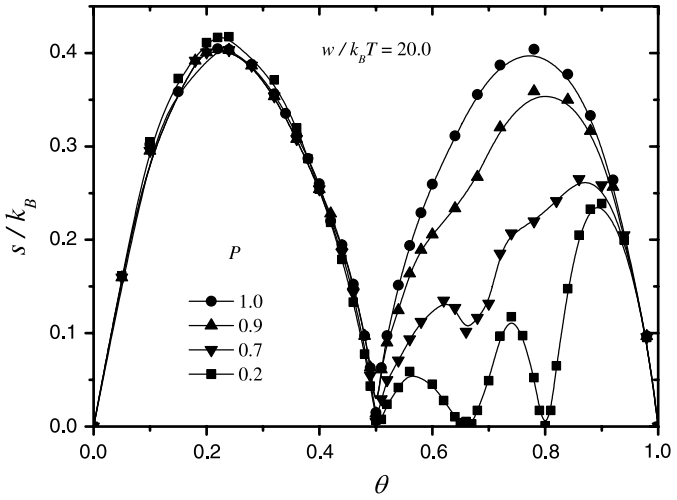

Fig. 3. Configurational entropy per site for monomers adsorbed on square lattices, $w/k_BT = 20$ and different values of the non-additivity parameter P, as indicated.

to $\theta = 1/2$ which corresponds to the systems without interactions (Langmuir case: lattice gas without lateral interactions). As the temperature decreases, the symmetry around half coverage is broken. The entropy tends to zero at the coverage where the ordered structures are formed and where the plateaus in the isotherms appear. These minima are deeper upon decreasing the temperature (always below the critical point, i.e. at $P = 1$, $k_BT_c/w = 0.567$). For a more clear analysis, different adsorption regimes can be defined for $T < T_c$:

(a) $0 \leq \theta \leq 1/2$: the particles adsorb in such a way as to avoid the occupation of nearest-neighbor (NN) sites. In this regime, the $c(2 \times 2)$ structure, which corresponds to an ordered lattice gas phase (or, in magnetic language, to the AF ordered two-dimensional phase), begins to be formed (see Table 1). The entropy shows a maximum around $\theta = 1/4$ at low temperatures.
(b) $1/2 \leq \theta \leq 2/3$: in this regime the structure $c(2 \times 2)$ begins to be destroyed and the entropy increases until it reaches a maximum, which depends on T. Then, the entropy falls because a new structure is formed at 2/3 monolayer coverage. This structure is characterized by domains of parallel "*zig–zag*" strips oriented at $\pm 45°$ from the lattice symmetry axes, separated from each other by strips of single empty sites (see Table 1).
(c) $2/3 \leq \theta \leq 4/5$: the situation is similar to (b), the only difference is the formation of the so-called "*tetrameric ordered structure*", because it resembles ordered tetramers on a square lattice (see Table 1).
(d) $4/5 \leq \theta \leq 1.0$: finally the entropy increases, goes to a maximum at $\theta = 0.88$ and decreases until the lattice is filled at full coverage.

It is of interest to know the behavior of the system below the critical point because in this range of temperatures all the new reported structures are formed. Fig. 3 shows the entropy versus surface coverage for different situations of non-additivity and at a fixed temperature $w/k_BT = 20.0$. At the additive situation, $P = 1.0$, the entropy is symmetric around $\theta = 1/2$, as a consequence of the equivalence between particle and vacancy. For all the cases considered, the entropy shows a maximum around $\theta = 1/4$. Because the interactions are weakening as P decreases, this maximum increases. In the situation $\theta > 1/2$, the corresponding minima for the new structures appear with different intensity, because the structures become stronger as $P < 1.0$. The minimum at $\theta = 2/3$, is more deep as the "*zig–zag structure*" is reinforced, which occurs as $P < 0.7$. The minimum for the "*tetrameric structure*" only appears as $P < 0.5$.

The configurational entropy is useful in order to estimate the influence of non-additive interactions on the critical temperature for the main structures formed. The entropy versus k_BT at the critical coverage presents an inflection point at T_c. This behavior is shown in inset (a) of Fig. 4, for $P = 0.7$. To identify the maximum, the derivative of the entropy with respect to the temperature is shown in inset (b) of Fig. 4. For the $c(2 \times 2)$ ordered phase (half coverage), the dependence of T_c on P can be calculated. Thus, Fig. 4 presents $T_c(P)$ (in units of critical temperature for the additive case, $k_BT_c/w = 0.567$) on the non-additive parameter. By means of a linear fit, one gets $T_c(P) = 0.10(2) + 0.47(2)P$. This nearly linear dependence is in complete agreement with previous work on adsorption thermodynamics [31]. Note that, for the additive case ($P = 1$), the critical temperature is the expected value.

Now, the behavior of the entropy for a system with the Hamiltonian given by Eq. (1) in a triangular lattice is analyzed. In Fig. 5, the entropy for $P = 0.2$ and different temperatures is shown. As the temperature begins to drop, a first minimum appears at $\theta = 2/3$, due to the $(\sqrt{\iota} \times \sqrt{\iota})^*$ ordered phase is formed. This low-temperature ordered phase has been already reported for additive systems [47]. Another minimum appears at $\theta = 1/3$, which corresponds to a $(\sqrt{\iota} \times \sqrt{\iota})$ ordered phase, also reported for additive systems. At very low temperature, other minima at $\theta = 2/5$, $1/2$, $3/4$ and $5/6$ can be identified (see Table 1). All these minima separate different adsorption regimes and determine the specific concentrations where new ordered structures appear, all of them in correspondence to those reported in a previous work [32].

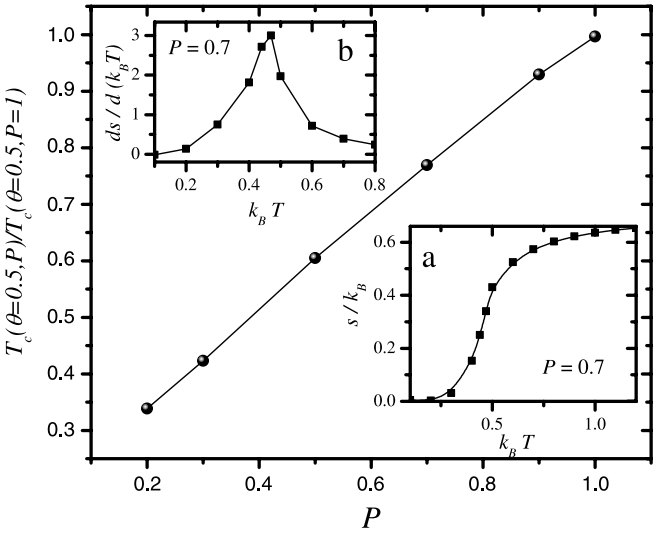

Fig. 4. Linear dependence of T_c versus P (in units of $T_c(P = 1)$) for the $c(2 \times 2)$ ordered phase. Inset (a): configurational entropy versus k_BT for $P = 0.7$. Inset (b): derivative of the configurational entropy with respect to temperature for the case shown in the inset (a).

Table 1
Typical snapshots of the low temperature phases for square, triangular and honeycomb lattices as indicated.

	Ordered phases
Square Lattice	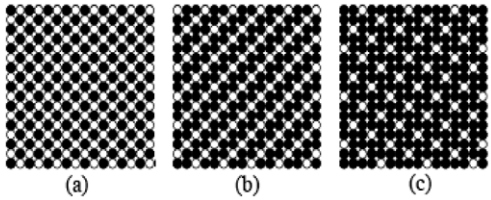 Ordered phases are plotted at: (a) $\theta = 1/2$, (b) $\theta = 2/3$ and (c) $\theta = 4/5$.
Triangular Lattice	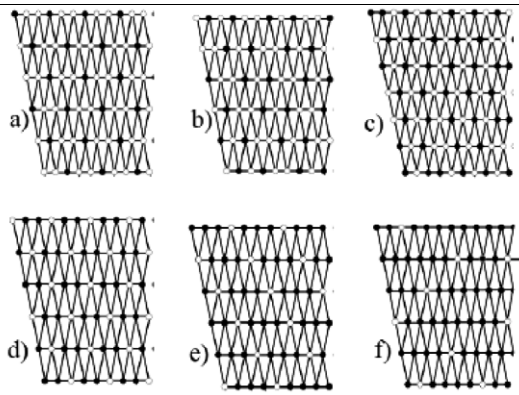 Ordered phases are plotted at: (a) $\theta = 1/3$, (b) $\theta = 2/5$, (c) $\theta = 1/2$, (d) $\theta = 2/3$, (e) $\theta = 3/4$ and (f) $\theta = 5/6$.
Honeycomb Lattice	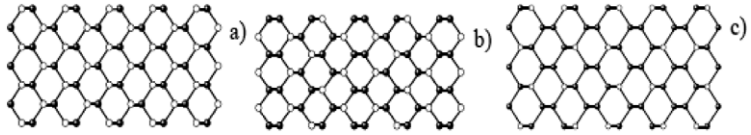 Ordered phases are plotted at: (a) $\theta = 1/2$, (b) $\theta = 5/8$ and (c) $\theta = 3/4$.

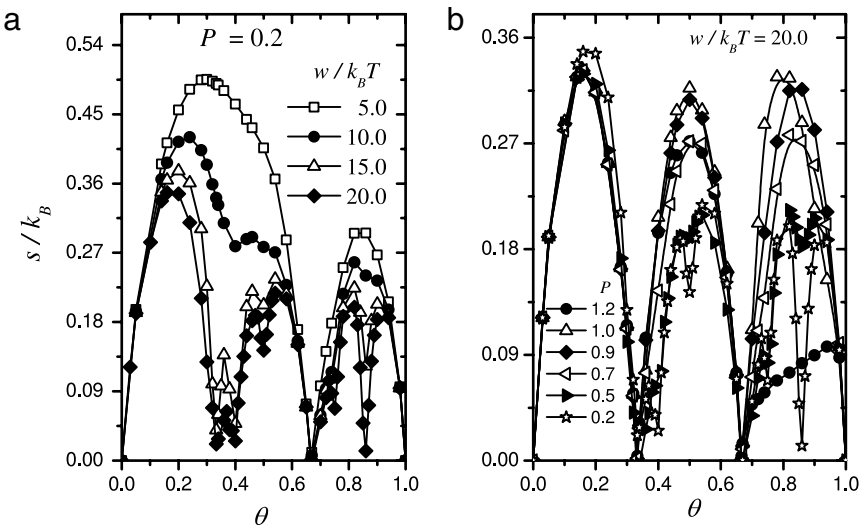

Fig. 5. Same as Fig. 2 for triangular lattices. The minima indicate the different structures formed in the adlayer.

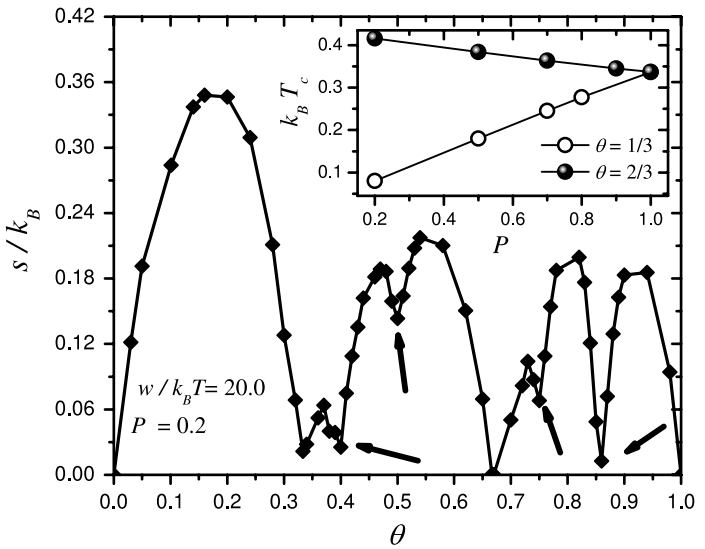

Fig. 6. Configurational entropy per site for monomers adsorbed on triangular lattices, $w/k_BT = 20.0$ and $P = 0.2$. The minima, indicating the different structures formed in the adlayer, are marked with arrows. The inset shows the variation of the critical temperature with the non-additive parameter for the $(\sqrt{\iota} \times \sqrt{\iota})$ and $(\sqrt{\iota} \times \sqrt{\iota})^*$ ordered phases.

To see that the minima of the entropy are a clear indication of the presence of the new ordered structures which were found through the analysis of the isotherms [32], in Fig. 6 the entropy for $P = 0.2$ is shown. The arrows are used to point out the minima corresponding to those structures. The dependence of the critical temperature with P is also estimated, at $\theta = 1/3$ and $\theta = 2/3$, with the same method used before (see inset in Fig. 6). T_c for $(\sqrt{\iota} \times \sqrt{\iota})[(\sqrt{\iota} \times \sqrt{\iota})^*]$ ordered phase decreases [increases] as a function of P in complete agreement with the isotherms analysis [32]. The $(\sqrt{\iota} \times \sqrt{\iota})[(\sqrt{\iota} \times \sqrt{\iota})^*]$ structure is weakened [strengthened] as P decreases [increases]. The linear fits for each structure in the inset of Fig. 6 are:

$$T_c = 0.32P + 0.01 \quad \text{for } \theta = 1/3 \quad \text{and}$$
$$T_c = -0.01P + 0.34 \quad \text{for } \theta = 2/3,$$

respectively. As it is expected, both lines tend to the same ordinate to the origin, T_c, in the additive condition.

Finally, in Fig. 7 the entropy for the honeycomb lattice, several values of P and low temperature are presented. The curves present minima at $\theta = 1/2, 5/8$ and $3/4$, which correspond to different ordered structures (see Table 1) [32]. The minimum for $\theta = 3/4$ only appears for $P < 0.7$. In the inset, the behavior of T_c at half coverage is shown. The linear fit is $T_c = 0.34P + 0.03$. As before, this behavior is in complete agreement with the conclusions drawn from the isotherms [32].

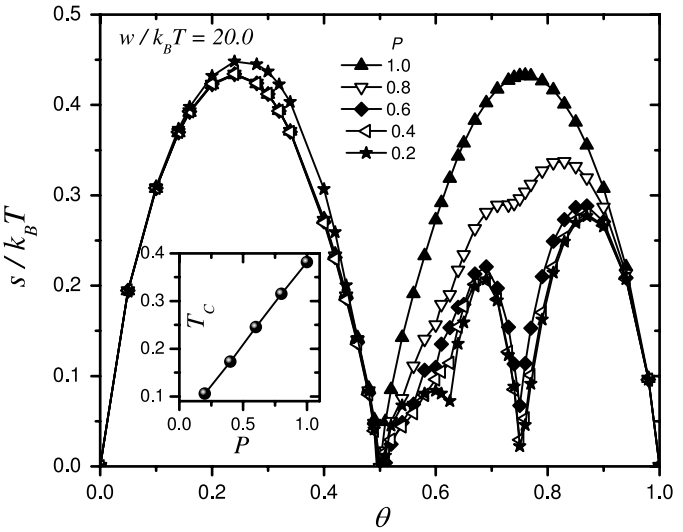

Fig. 7. Same as Fig. 2 for honeycomb lattices. The inset shows the variation of the critical temperature with the non-additive parameter for the ordered phase occurring at half coverage.

5. Conclusions

By using the thermodynamic integration method, the configurational entropy per site was calculated for a lattice gas of monomers adsorbed on square, triangular and honeycomb surfaces. The traditional and widely used assumption of additivity for the lateral interaction energy between adatoms was replaced by a more realistic one for several experimental systems: the energy between nearest neighbor depends on the state of occupation in the first coordination sphere of each adatom.

A non-additivity parameter P was introduced as a measure for the stronger to the weakest lateral coupling possible in each system. For the case P less than one, it is possible to identify minima in the configurational entropy per site at defined coverages where different ordered structures are formed in the adlayer. These minima allow us to conclude about the existence of low-temperature ordered phases in each one of the considered lattices, in complete agreement with previous results coming from the adsorption isotherms [31,32].

Finally, the critical temperatures corresponding to the different ordered phases occurring in the studied adlayers were estimated by plotting the configurational entropy per site (and its derivative) as a function of the temperature. The inflection on s/k_B (the peak in its derivative) determines the critical temperatures. In all cases, a nearly linear dependence of T_C with the non-additivity parameter was established. A more exact determination of T_C based on Monte Carlo simulations in the canonical ensemble and finite-size scaling theory will be the object of future studies.

Acknowledgments

This work was supported in part by CONICET (Argentina) under project no. PIP 112-200801-01332; the Universidad Nacional de San Luis (Argentina) under project 322000 and the National Agency of Scientific and Technological Promotion (Argentina) under project PICT-2010-1466. All calculations were done using the parallel cluster BACO2 of Universidad Nacional de San Luis, Argentina. This facility consists of 50 PCs each with an Intel Core i7 processor running at 2.93 GHz and 512 MB of RAM per core.

References

[1] G. Ertl, J. Kuppers, Surf. Sci. 21 (1970) 61.
[2] G. Ertl, D. Schillinger, J. Chem. Phys. 66 (1977) 2569.
[3] W.Y. Ching, D.L. Huber, M. Fishkis, M.G. Legally, J. Vac. Sci. Technol. 15 (1987) 417.
[4] W.Y. Ching, D.L. Huber, M.G. Legally, G.C. Wang, Surf. Sci. 77 (1978) 550.
[5] F. Boszo, G. Ertl, M. Grunze, M. Weiss, Appl. Surf. Sci. 1 (1979) 103.
[6] R. Imbihl, R.J. Behm, K. Christmann, G. Ertl, T. Matsushima, Surf. Sci. 117 (1982) 257.
[7] W. Kinzel, W. Selke, K. Binder, Surf. Sci. 121 (1982) 13.
[8] M.C. Giménez, E.P.M. Leiva, Langmuir 19 (2003) 10538.
[9] M.I. Rojas, M.C. Giménez, E.P.M. Leiva, Surf. Sci. Lett. 581 (2005) L109.
[10] M.C. Giménez, E.V. Albano, J. Phys. Chem. C 111 (2007) 1809.
[11] M.C. Giménez, M.G. del Pópolo, E.P.M. Leiva, Electrochim. Acta 45 (1999) 699.
[12] M.C. Giménez, M.G. del Pópolo, E.P.M. Leiva, S.G. Garca, D.R. Salinas, C.E. Mayer, W.J. Lorenz, J. Electrochem. Soc. 149 (2002) E109.
[13] M.C. Giménez, M.G. del Pópolo, E.P.M. Leiva, Langmuir 18 (2002) 9087.
[14] T.L. Hill, An Introduction to Statistical Thermodynamics, Addison Wesley, Reading, 1962.
[15] A. Boutin, R.J.-M. Pellenq, D. Nicholson, Chem. Phys. Lett. 219 (1994) 484.

[16] V. Lachet, A. Boutin, R.J.-M. Pellenq, D. Nicholson, A.H. Fuchs, J. Phys. Chem. 100 (1996) 9006.
[17] R. Radhakrishnan, K. Gubbins, Phys. Rev. Lett. 79 (1997) 2847.
[18] T. Maris, T.J.H. Vlugt, B. Smit, J. Phys. Chem. 102 (1998) 7183.
[19] C. Martin, N. Tosi-Pellenq, J. Patarin, J.P. Coulomb, Langmuir 14 (1998) 1774.
[20] P.A. Rikvol, K. Kaski, J.D. Gunton, M.C. Yalabik, Phys. Rev. B 29 (1984) 11.
[21] W.H. Ching, D. Huber, M.G. Lagally, G.-C. Wang, Surf. Sci. 77 (1979) L497.
[22] K. Binder, D.P. Landau, Surf. Sci. 108 (1981) 503.
[23] L.C.A. Stoop, Thin Solid Films 103 (1983) 375.
[24] K. Kaski, W. Kinzel, J.D. Gunton, Phys. Rev. B 27 (1983) 6777.
[25] P.A. Rikvold, K. Kaski, J.D. Gunton, M.C. Yalabik, Phys. Rev. B 29 (1984) 6285.
[26] J. Kolaczkiewicz, E. Bauer, Surf. Sci. 151 (1985) 333.
[27] T.L. Einstein, Langmuir 7 (1991) 2527.
[28] A. Milchev, M. Paunov, Surf. Sci. 108 (1981) 25.
[29] A. Milchev, Electrochim. Acta 28 (1983) 941.
[30] A. Milchev, K. Binder, Surf. Sci. 164 (1985) 1.
[31] O.A. Pinto, A.J. Ramirez-Pastor, F. Nieto, Surf. Sci. 602 (2008) 1763.
[32] O.A. Pinto, A.J. Ramirez-Pastor, F. Nieto, Physica A 389 (2010) 3456.
[33] O.A. Pinto, P.M. Pasinetti, A.J. Ramirez-Pastor, F. Nieto, J. Chem. Phys. 134 (2011) 064702.
[34] J.P. Hansen, L. Verlet, Phys. Rev. 184 (1969) 151.
[35] K. Binder, J. Stat. Phys. 24 (1981) 69.
[36] K. Binder, Z. Phys. B: Condens. Matter. 45 (1981) 61.
[37] F. Romá, A.J. Ramirez-Pastor, J.L. Riccardo, Langmuir 16 (2000) 9406.
[38] F. Romá, A.J. Ramirez-Pastor, J.L. Riccardo, J. Chem. Phys. 114 (2001) 10932.
[39] F. Romá, A.J. Ramirez-Pastor, Physica A 328 (2003) 513.
[40] P.M. Pasinetti, J.L. Riccardo, A.J. Ramirez-Pastor, J. Chem. Phys. 122 (2005) 154708.
[41] A.M. Ferrenberg, D.P. Landau, Phys. Rev. B 44 (1991) 5081.
[42] K. Binder, Applications of the Monte Carlo Method in Statistical Physics, in: Topics in Current Physics, vol. 36, Springer, Berlin, 1986.
[43] N. Metrópolis, S. Ullam, J. Amer. Statist. Assoc. 44 (1949) 335.
[44] N. Metropolis, A.W. Rosenbluth, M.N. Rosenbluth, A.H. Teller, E. Teller, J. Chem. Phys. 21 (1953) 1087.
[45] K. Kawasaki, Phys. Rev. 145 (1966) 224.
[46] K. Hukushima, K. Nemoto, J. Phys. Soc. Japan 65 (1996) 1604.
[47] R.J. Baxter, Exactly Solved Models in Statistical Mechanics, Academic, London, 1982.